

Origin of the 4.1-eV luminescence in pure CsI scintillator

H. Nishimura, M. Sakata, T. Tsujimoto, and M. Nakayama

Department of Applied Physics, Faculty of Engineering, Osaka City University, Sugimoto, Sumiyoshi-ku, Osaka 558, Japan

(Received 28 July 1994)

The spectra and decay times of the 4.3- and 3.7-eV luminescence bands associated with the self-trapped excitons (STE's) in CsI have been observed in a wide temperature range (4.5–300 K) by using two-photon spectroscopy. The results reveal that the 4.1-eV luminescence in pure CsI, which is well known as the room-temperature scintillation, appears mainly from the 4.3-eV STE state: the 4.3-eV STE luminescence is dominant below 6 K and is quenched above 6 K, but appears again at 4.1 eV at room temperature by thermal activation of STE's from the 3.7-eV STE state to the 4.3-eV STE state.

I. INTRODUCTION

Pure CsI, which has been known to emit the 4.1-eV luminescence with a short decay time (15 ns) at room temperature, has been extensively investigated from the viewpoint of possible applications as a scintillator with fast timing characteristics.^{1–8} The origin of the 4.1-eV luminescence is, however, still controversial; the question of whether it is intrinsic or extrinsic is still unanswered. There are several interpretations proposed for its origin: (1) an interatomic transition between the $I^- (5p^6)$ valence band and the $Cs^+ (5p^6)$ core band,⁵ (2) a radiative decay of free excitons trapped by defects,⁸ and (3) a radiative decay of the self-trapped excitons (STE's) responsible for the 3.7-eV luminescence band.^{1,4}

In CsI, there are two types of STE states responsible for the 4.3- and 3.7-eV luminescence bands. Iida *et al.*⁹ proposed that the STE states can be represented by linear combinations of the $5p$ orbitals of two nearest-neighbor I^- ions and by those of the $6s$ and $5d$ orbitals of the 12 neighboring Cs^+ ions. Assuming this cluster with the D_{4h} symmetry, they have assigned the 4.3-eV band to the ${}^3\Gamma_4^-$ state composed of the $5d$ orbital, and the 3.7-eV band to the ${}^3\Gamma_2^-$ state composed of the $6s$ orbital. Recently, Tsujimoto *et al.*¹⁰ studied the hydrostatic pressure effects on the 4.3- and 3.7-eV bands, and concluded that the 4.3-eV band does not arise from the ${}^3\Gamma_4^-$ state; it arises from the on-center configuration of the ${}^3\Gamma_2^-$ state, and the 3.7-eV band arises from the off-center configuration of the same ${}^3\Gamma_2^-$ state.

In the present study, we have measured the spectra and decay times of the 4.3- and 3.7-eV bands in a wide temperature range (4.5–300 K) by using two-photon spectroscopy. From the results, we have concluded that the STE's in CsI are thermally populated both on the on-center and off-center STE states at room temperature, and emit the 4.1-eV luminescence mainly from the on-center STE state with a larger radiative decay rate.

II. EXPERIMENTAL PROCEDURES

The pure CsI crystal used in the present study was obtained from the Harshaw Chemical Co. Samples with a

typical dimension of $5 \times 5 \times 2$ mm³ were cooled by heat conduction. We used a conventional method for the two-photon spectroscopy. A tunable dye laser (PRA LN-102) pumped by a pulsed nitrogen-gas laser (PRA LN-100) with the peak power of 250 kW was used as the light source. The time duration of the dye laser pulse (we used 4,4''-bis-butylacetoxy-*o*-terphenyl as the dyestuff) is shorter than 1 ns. We used a quartz-prism monochromator (Carl Zeiss M4QIII) and a photomultiplier tube (Hamamatsu R-955) for the measurement of luminescence spectra, and a box-car integrator (Stanford SR-250) for time-resolved spectra. Luminescence decay times were measured by using a 500-MHz digitizing oscilloscope (Tektronix TDS-520) and a photomultiplier tube (Hamamatsu R-1546). The time resolution of the detecting system was 1 ns. Luminescence spectra were corrected for the sensitivity of the detecting system.

III. EXPERIMENTAL RESULTS

Figure 1 shows the luminescence spectra of a pure CsI crystal observed at various temperatures in the two-photon absorption of 3.18-eV light. The 4.3-eV band is dominant at 4.5 K, but it is reduced abruptly above 6 K, while the 3.7-eV band is enhanced, keeping total intensity constant. This result is consistent with the result obtained in the one-photon absorption.¹¹ In the present study, we found that the 4.3-eV band is still observable even at 80 K, and is enhanced again above 85 K. The integrated intensities of the 4.3- and 3.7-eV bands are shown in Fig. 2 as a function of temperature. It is noted that the total intensity of these two bands decreases gradually above 80 K. Figure 1 shows also that the peak energy of the 4.3-eV band shifts to lower energy and reaches 4.1 eV at 290 K, and that of the 3.7-eV band shifts to higher energy, as temperature rises.

Figures 3 and 4 show the decay times of the 4.3- and 3.7-eV bands as a function of temperature. The decay time of the 4.3-eV band has been reported to be 100 ns at 5 K.¹¹ As shown in Figs. 3 and 5(a), however, the 4.3-eV band has a 2-ns component in addition to the 100-ns component at 5 K. The integrated intensity ratio of the former to the latter is 0.02. The decay time of the 100-ns component decreases abruptly above 6 K in accordance

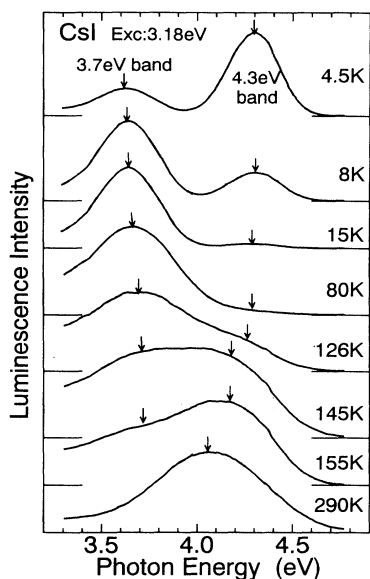


FIG. 1. Spectra of the 4.3- and 3.7-eV bands at various temperatures in the two-photon absorption of 3.18-eV light. Arrows show the peak positions of the two bands. The peak positions of the complex band at high temperature are found by dividing the band into two Gaussian bands.

with the intensity decrease, while that of the 2-ns component remains constant until 160 K. Figure 5(b) shows clearly that the weak 4.3-eV band at 80 K is composed of the 2-ns component only. Figures 3 and 4 show that a little slower component (30 ns at 200 K) appears in the 4.3-eV band above 200 K. The decay time of this component decreases with increasing temperature and reaches 15 ns at 290 K. Furthermore, a much slower component (1 μ s at 85 K) appears above 85 K in the 4.3-eV band. The decay time of this component also decreases with increasing temperature. These two slowly decaying components are observed also in the 3.7-eV band.

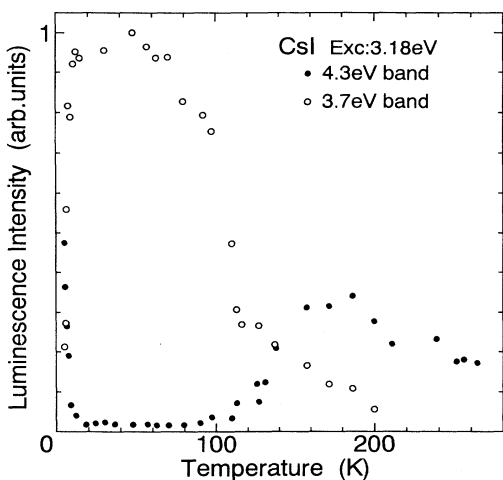


FIG. 2. Integrated intensities of the 4.3- and 3.7-eV bands excited by 3.18-eV light as a function of temperature.

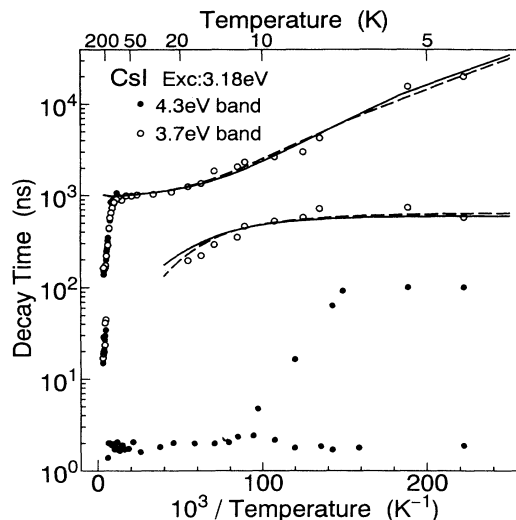


FIG. 3. Decay times of the 4.3- and 3.7-eV bands as a function of temperature. The solid and broken curves are the best fits of the two exponential decay terms of n_s in the one-phonon and two-phonon processes, respectively.

The 3.7-eV band is composed of the 0.6- and 20- μ s components at 5 K as shown in Figs. 3 and 6(a). The integrated intensity ratio of the former to the latter is 0.2, and the 0.6- μ s component disappears above 20 K. The decay time of the 20- μ s component decreases with increasing temperature and reaches a plateau of 1 μ s at 20 K (Figs. 3 and 4). The decay curves of the 3.7-eV band show a remarkable delay below 160 K as shown in Figs. 6(a) and 6(b), and above 160 K the decay curve becomes quite similar to that of the 4.3-eV band [Fig. 6(c)].

Figure 7 shows the time-resolved spectra of the 4.3-

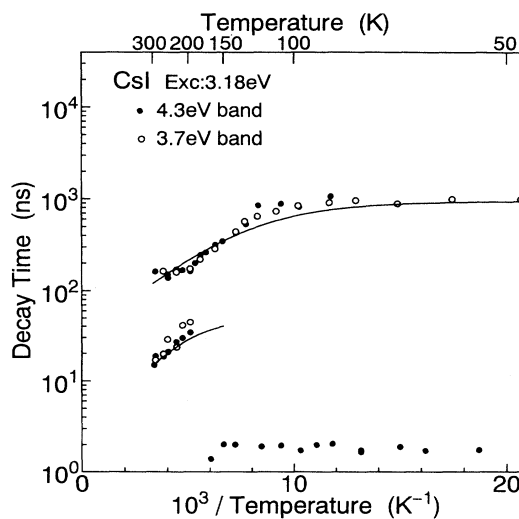


FIG. 4. Decay times of the 4.3- and 3.7-eV bands above 50 K. The solid curves are the best fits of Eq. (3) to the data for the singlet and triplet STE's.

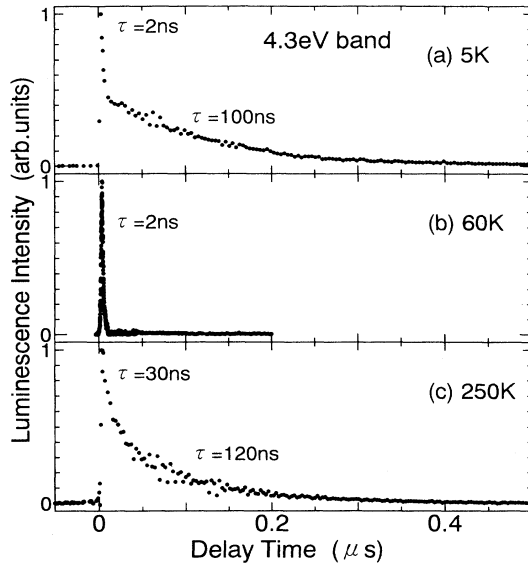


FIG. 5. Decay curves of the 4.3-eV band at three temperatures.

and 3.7-eV bands. These spectra show that (1) the 2- and 100-ns components of the 4.3-eV band have the same spectral distribution at 4.5 K, (2) the 100-ns component is not seen at 80 K, consistent with the result in Fig. 5(b), and (3) the 4.3-eV band includes a slowly decaying component above 85 K. Fact (3) suggests that a thermal activation of STE's occurs from the 3.7-eV state to the 4.3-eV state.

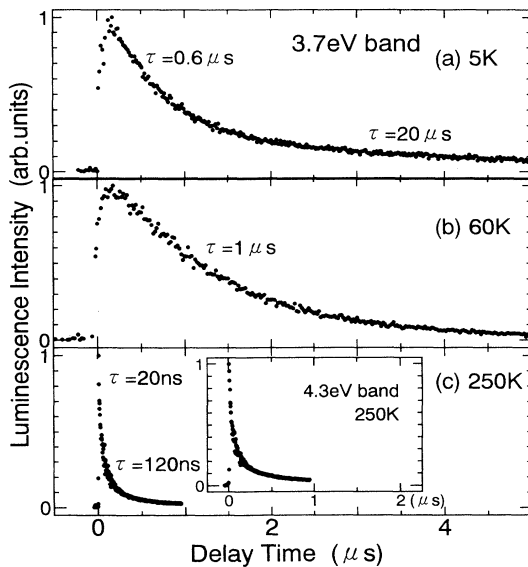


FIG. 6. Decay curves of the 3.7-eV band at three temperatures.

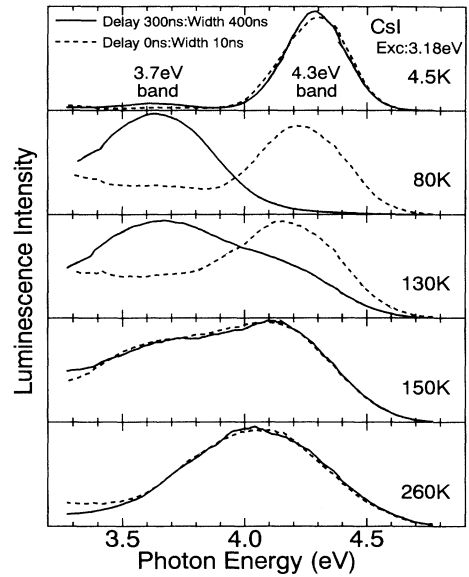


FIG. 7. Time-resolved spectra of the 4.3- and 3.7-eV bands at various temperatures in the two-photon absorption of the 3.18-eV light. Broken curves are obtained by 0-ns delay and 10-ns width, and solid curves by 300-ns delay and 400-ns width.

IV. DISCUSSION

In a pure CsI, a majority of free holes created in the two-photon absorption are self-trapped in a very short time ($\ll 1$ ns). A self-trapped hole captures a free electron to form a STE with a high efficiency. Iida *et al.*^{9,12,13} concluded that the initial state for the 4.3-eV band is the Γ_4^- state. However, the 2-ns component of the 4.3-eV band is not assignable to the singlet ${}^1\Gamma_4^- \rightarrow {}^1\Gamma_1^+$ transition, because it is forbidden.⁹ Thus, the 2-ns component should be assigned to the singlet ${}^1\Gamma_2^- \rightarrow {}^1\Gamma_1^+$ transition, and the 100-ns component of the 4.3-eV band to the triplet ${}^3\Gamma_2^- \rightarrow {}^1\Gamma_1^+$ transition. This assignment is consistent with the result reported by Pellaux *et al.*¹³ They observed that the 4.3-eV band is π polarized at 5 K and σ polarized above 11 K. This result suggests that the 100-ns component dominant below 6 K is π polarized and assignable to the ${}^3\Gamma_2^- \rightarrow {}^1\Gamma_1^+$ transition, while the 2-ns component dominant above 11 K is σ polarized and assignable to the ${}^1\Gamma_2^- \rightarrow {}^1\Gamma_1^+$ transition.

We thus conclude that the initial state for the 4.3-eV band is not the Γ_4^- state but the Γ_2^- state. Since no other state assignable to the 3.7-eV band exists, we further propose that the initial state for the 3.7-eV band is also the Γ_2^- state; however, it is in the off-center configuration, and the state for the 4.3-eV band is in the on-center configuration. The same conclusion has been obtained by Tsujimoto *et al.*¹⁰ in a hydrostatic pressure experiment on the 4.3- and 3.7-eV bands.

Recent studies on the STE's in alkali halides have concluded that an off-center configuration for the STE is occasionally stable.¹⁴⁻²¹ We propose the on-center and

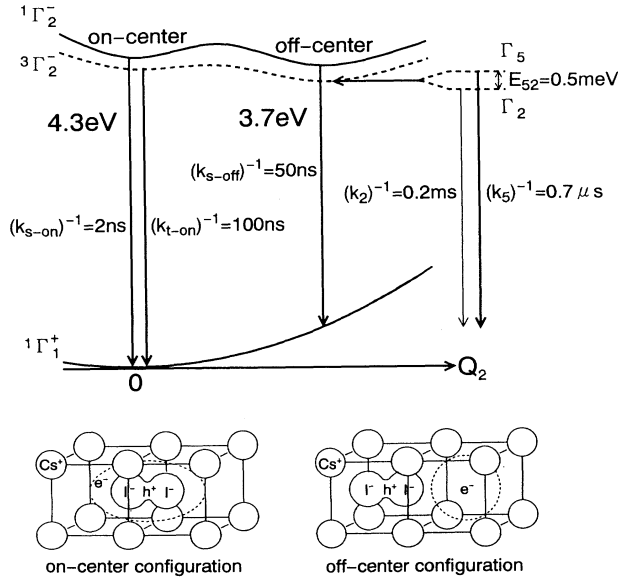


FIG. 8. A diagram of the adiabatic potential-energy surfaces for the singlet and triplet STE states in CsI. The surfaces are cut along the Q_2 coordinate representing an off-center relaxation. The on-center and off-center configurations are depicted under the diagram.

off-center configurations in CsI, as depicted in Fig. 8. The on-center configuration is composed of an electron trapped by a V_k center (I_2^-), in which the electron and hole are populated on the I_2^- center with the D_{4h} symmetry, while the off-center configuration is composed of a nearest-neighbor pair of F and H centers, in which the electron and hole are separated from each other to form the Frenkel pair (F and H pair) with the C_{4v} symmetry. We also show a diagram of the adiabatic potential-energy surfaces of the singlet and triplet STE states in Fig. 8, which depicts what we suppose is happening in CsI. The energy surfaces are cut along the off-center axis Q_2 .

We then assign the two slowly decaying components (0.6 and 20 μ s) of the 3.7-eV band to the triplet $3\Gamma_2^- \rightarrow 1\Gamma_1^+$ transition in the off-center configuration. A quickly decaying component, which is expected to arise from the singlet $1\Gamma_2^- \rightarrow 1\Gamma_1^+$ transition in the off-center configuration, is not seen in the 3.7-eV band. This singlet component is probably weak as it is in the on-center configuration, and it may be obscure in the delay part of the slowly decaying components [Fig. 6(a) and 6(b)].

Next, we discuss the 0.6- and 20- μ s components of the

3.7-eV band in detail. As shown in Fig. 3, the decay time of the slower component decreases exponentially from 20 μ s at 5 K to 1 μ s at 20 K, while that of the other component (0.6 μ s) is independent of temperature. These results are interpretable in terms of changing populations of STE's in the triplet states. The $3\Gamma_2^-$ state splits into two sublevels by the spin-orbit interaction: Γ_5^- and Γ_1^- states in the on-center STE with D_{4h} symmetry, and Γ_5 and Γ_2 states in the off-center STE with C_{4v} symmetry. The Γ_5 state is a mixture of the triplet and singlet states, and the Γ_1^- and Γ_2 states are of pure triplet. Thus, the STE's populated on the Γ_5 state decay radiatively with π polarization, while the STE's populated on the Γ_2 state decay mainly through the Γ_5 state.

We first assume the STE populations on the Γ_5 and Γ_2 states, n_5 and n_2 , to decay in accordance with the following rate equations based on the one-phonon process:

$$dn_5/dt = -n_5\{k_5 + k_{52}(\bar{n} + 1)\} + n_2 k_{25} \bar{n}, \quad (1)$$

$$dn_2/dt = -n_2(k_2 + k_{25}\bar{n}) + n_5 k_{52}(\bar{n} + 1), \quad (2)$$

where \bar{n} represents the phonon occupation number: $\{\exp(E_{52}/k_B T) - 1\}^{-1}$, E_{52} is the energy separation between the Γ_5 and Γ_2 states, k_5 and k_2 are the decay rates from the Γ_5 and Γ_2 states to the ground state, k_{52} and k_{25} are the transition rates of STE's from the Γ_5 state to the Γ_2 state, and the reverse. Solving Eqs. (1) and (2) under an initial condition ($n_5 = n_0$ and $n_2 = 0$ at $t = 0$), we obtain n_5 to be given by the sum of two exponential decay terms. The solid curves in Fig. 3 represent the best fits of these two decay terms to the data. The values of several parameters obtained by the fittings are given in Table I(A). Some of these values are close to those obtained by Lamatsch, Rossel, and Saurer¹¹ in a thermal-activation model, given in Table I(C). Fischbach, Frohlich, and Kabler²² have first discussed the data of Lamatsch, Rossel, and Saurer in the model based on the one-phonon process.

The data in Table I(A), however, gives an unreasonably large value 12.6 for k_{25}/k_{52} , which should be 2 on account of the ratio of the statistical weight of each final state. Furthermore, the value of 2 meV for E_{52} is much larger than the value 0.495 meV obtained by Falco *et al.*¹² in an experiment of the magnetic circular polarization. In order to resolve these discrepancies, we adopt the Orbach model instead of the above model. In the Orbach model, the transitions between the Γ_5 and Γ_2 states are assumed to occur in a two-phonon process via an intermediate state lying above these two states. We assume the intermediate state I to be the $1\Gamma_2^-$ singlet state. In this

TABLE I. The values of several parameters obtained in the model based on the one-phonon process (A) and those obtained in the model based on the two-phonon process (B), and those reported by Lamatsch, Rossel, and Saurer (Ref. 11) (C).

	E_{52}	E_{51}	E_{21}	k_5^{-1}	k_2^{-1}	k_{52}^{-1}	k_{25}^{-1}	k_{25}/k_{52}
A	2 meV			0.9 μ s	70 μ s	1.8 μ s	0.14 μ s	12.6
B	0.5 meV	0.9 meV	1.4 meV	0.7 μ s	0.2 ms	1.7 μ s	0.7 μ s	2.4
C	2 meV			0.6 μ s	65 μ s			

case, $k_{52}(\bar{n}+1)$ and $k_{25}\bar{n}$ in Eqs. (1) and (2) are replaced by $k_{52}\bar{n}_{51}(\bar{n}_{21}+1)$ and $k_{25}\bar{n}_{21}(\bar{n}_{51}+1)$, respectively.²³ Here, $\bar{n}_{51}=\{\exp(E_{51}/kT)-1\}^{-1}$ and $\bar{n}_{21}=\{\exp(E_{21}/kT)-1\}^{-1}$, and E_{51} and E_{21} are the energy difference between the Γ_5 and I states and between the Γ_2 and I states, respectively. Fitting the solutions of these equations to the data (broken curves in Fig. 3), we obtain the improved values for k_{25}/k_{52} and E_{52} to be 2.4 and 0.5 meV, respectively. The values obtained for several parameters in the Orbach model are given in Table I (B).

A thermal activation of STE's from the off-center state to the on-center state is likely to occur on the triplet surface at high temperatures, since both the 4.3- and 3.7-eV bands have a common slowly decaying component above 85 K (1 μ s at 85 K), and since the intensity of the 4.3-eV band increases at the expense of the 3.7-eV band intensity. Keeping this in mind, and taking into account the much larger decay rate of the triplet transition in the on-center configuration (0.1 μ s)⁻¹ than in the off-center one (0.7 μ s)⁻¹, we conclude that the stronger intensity for the 4.3-eV band than for the 3.7-eV band above 150 K is reasonable.

Similar thermal activation of STE's is likely to occur on the singlet surface, since the 4.3- and 3.7-eV bands have a common quickly decaying component above 200 K (30 ns at 200 K), and since the decay time decreases with increasing temperature. In this case, the radiative transition occurs mainly through the on-center configuration with a larger decay rate rather than through the off-center one, so that the decay time decreases with increasing temperature.

Assuming a Boltzmann distribution for the on-center and off-center STE's, $n_{\text{on}}/n_{\text{off}}=\exp(-E_d/kT)$, and assuming a weak nonradiative decay with a rate of $k_n\exp(-E_a/kT)$ for the on-center STE's, we obtain a mean-decay rate τ^{-1} of the STE's on the singlet surface and on the triplet surface to be

$$\tau^{-1}=\frac{\exp(-E_d/kT)\{k_{\text{on}}+k_n\exp(-E_a/kT)\}+k_{\text{off}}}{\exp(-E_d/kT)+1}, \quad (3)$$

where E_d represents the energy difference between the on-center and off-center STE states, and k_{on} and k_{off} the radiative decay rates of the on-center and off-center STE's. The solid curves in Fig. 4 represent the best fits of Eq. (3) to the data for the singlet and triplet transitions. The values of several parameters obtained by the fittings are given in Table II.

The nonradiative decay is probably caused by the hopping motion of the on-center STE's, because strong impurity bands increase at the expense of the 4.3- and 3.7-

eV band intensities at high temperatures. For the off-center STE's with less symmetry and thus with larger activation energy than for the on-center STE's,²⁴ the hopping motion seems hardly to occur.

The decay times that we estimated for the singlet and triplet transitions are shorter in the on-center configuration ($\tau_s=2$ ns and $\tau_t=100$ ns) than in the off-center one ($\tau_s=50$ ns and $\tau_t=0.7-0.9$ μ s). These results are reasonable, because the overlapping of the electron and hole wave functions are larger in the on-center configuration than in the off-center one.^{21,25,26}

The red shift of the 4.3-eV band and the blue shift of the 3.7-eV band (Fig. 1) suggest also that the 4.3-eV band arises from an on-center STE and the 3.7-eV band from an off-center STE, since in most alkali halides with the NaCl structure, the STE luminescence bands arising from on-center STE's are known to show a red shift, and the STE luminescence bands arising from off-center STE's show a blue shift.^{27,28}

As shown in Figs. 3 and 4, the quenching temperature of the 4.3-eV band is very much lower for the 100-ns triplet component (6 K) than for the 2-ns singlet component (160 K). This result suggests that the potential barrier height between the on-center and off-center configurations is much smaller on the triplet surface than on the singlet surface. This may be reasonable because the triplet states in most alkali halides with the NaCl structure are proposed to be metastable or unstable in the on-center configuration by Kayanuma.¹⁸ This means that the potential depth at $Q_2=0$ is much shallower on the triplet surface than on the singlet surface.

It has been reported that the 4.1-eV band is not excited by the photons in the fundamental absorption region.⁵ In the present study, we also have found that the 4.3- and 3.7-eV bands are not excited above 160 K in the one-photon absorption, and both bands are replaced by strong impurity bands. Probably the STE's formed near the crystal surface in the one-photon absorption move by hopping motion at high temperatures and decay at defects, which are mostly populated near the crystal surface. In the two-photon absorption, on the other hand, a lot of STE's are formed inside the crystal and, thus, they can decay radiatively before they are captured by the defects. As shown in Fig. 2, however, the total intensity of the 4.3- and 3.7-eV bands decreases gradually above 80 K. This result suggests that the nonradiative decay rate caused by the STE hopping motion becomes large above 80 K even in the case of the two-photon absorption.

Schotanus, Kamermans, and Dorenbus⁷ reported that the 4.1-eV band includes a long decay-time component (1 μ s) at room temperature. According to them, the integrated intensity of this component is about 50% of the total intensity, and depends on the method of excitation. We have observed that this component is excited also in the two-photon absorption, but the time-resolved spectrum is different from those of the other components: the spectrum of the 1- μ s component is spread over a wide energy region (4.6-3 eV). We thus exclude this component from the intrinsic 4.1-eV luminescence.

In conclusion, the singlet and triplet STE states in CsI are stable both in the on-center and off-center

TABLE II. The values of several parameters in Eq. (3), obtained by the fittings of Eq. (3) to the data in Fig. 4.

	k_{on}^{-1}	k_{off}^{-1}	E_d	k_n^{-1}	E_a
Singlet	2 ns	50 ns	60 meV	2 ns	60 meV
Triplet	100 ns	0.9 μ s	25 meV	20 ns	25 meV

configurations. The STE's are in thermal equilibrium at high temperatures both on the singlet and triplet surfaces. The 4.1-eV band in pure CsI scintillator arises mainly from the on-center configuration. The quickly de-

caying component (15 ns at 290 K) is assignable to the singlet ${}^1\Gamma_2^- \rightarrow {}^1\Gamma_1^+$ transition, and the slowly decaying component (100 ns at 290 K) to the triplet ${}^3\Gamma_2^- \rightarrow {}^1\Gamma_1^+$ transition in the on-center configuration.

-
- ¹R. Gwin and R. B. Murray, *Phys. Rev.* **131**, 508 (1963).
²W. Rehm and A. Scharmann, *Z. Naturforsch Teil A* **21**, 666 (1966).
³T. Towiyama, I. Morita, and M. Ishiguro, *J. Phys. Soc. Jpn.* **25**, 1133 (1968).
⁴C. H. Chen, M. P. McCann, and J. C. Wang, *Solid State Commun.* **61**, 559 (1987).
⁵S. Kubota, S. Sakuragi, S. Hashimoto, and J. Ruan (Gen), *Nucl. Instrum. Methods A* **268**, 275 (1988).
⁶B. K. Utts and S. E. Spagno, *IEEE Trans. Nucl. Sci.* **37**, 134 (1990).
⁷P. Schotanus, R. Kamermans, and P. Dorenbos, *IEEE Trans. Nucl. Sci.* **37**, 177 (1990).
⁸M. Abdrakhmanov, S. Chernov, R. Deich, and V. Gavrilov, *J. Lumin.* **54**, 197 (1992).
⁹T. Iida, Y. Nakaoka, J. P. von der Weid, and M. A. Aegerter, *J. Phys. C* **13**, 983 (1980).
¹⁰T. Tsujimoto, H. Nishimura, M. Nakayama, H. Kurisu, and T. Komatsu, *J. Lumin.* **60&61**, 798 (1994).
¹¹H. Lamatsch, J. Rossel, and E. Saurer, *Phys. Status Solidi B* **48**, 311 (1971).
¹²L. Falco, J. P. von der Weid, M. A. Aegerter, T. Iida, and Y. Nakaoka, *J. Phys. C* **13**, 993 (1980).
¹³J. P. Pellaux, T. Iida, J. P. von der Weid, and M. A. Aegerter, *J. Phys. C* **13**, 1009 (1980).
¹⁴D. Block, A. Wasiela, and Y. Merle d'Aubigne, *J. Phys. C* **11**, 4201 (1978).
¹⁵C. H. Leung, G. Brunet, and K. S. Song, *J. Phys. C* **18**, 4459 (1985).
¹⁶R. T. Williams, K. S. Song, W. L. Faust, and C. H. Leung, *Phys. Rev. B* **33**, 7232 (1986).
¹⁷R. T. Williams and K. S. Song, *J. Phys. Chem. Solids* **151**, 679 (1990).
¹⁸Y. Kayanuma, *Rev. Solid State Sci.* **4**, 403 (1990).
¹⁹K. Kan'no, K. Tanaka, and T. Hayashi, *Rev. Solid State Sci.* **4**, 383 (1990).
²⁰K. Tanimura, S. Suzuki, and N. Itoh, *Phys. Rev. Lett.* **68**, 635 (1992).
²¹K. S. Song and R. T. Williams, *Self-Trapped Excitons* (Springer-Verlag, Berlin, 1992).
²²J. U. Fischbach, D. Frohlich, and M. N. Kabler, *J. Lumin.* **6**, 29 (1973).
²³R. Orbach, *Proc. R. Soc. London Ser. A* **264**, 458 (1961).
²⁴L. F. Chen and K. S. Song, *Nucl. Instrum. Methods B* **46**, 216 (1990).
²⁵K. S. Song and L. F. Chen, *J. Phys. Soc. Jpn.* **58**, 3022 (1989).
²⁶R. T. Williams, Hanli Liu, G. P. Williams, Jr., and K. J. Platt, *Phys. Rev. Lett.* **66**, 2140 (1991).
²⁷S. Suzuki, K. Tanimura, N. Itoh, and K. S. Song, *J. Phys. Condens. Matter* **1**, 6993 (1989).
²⁸H. Nishimura, in *Direction in Condensed Matter Physics, Defect Processes Induced by Electronic Excitation in Insulators* Vol. 5, edited by N. Itoh (World Scientific, Singapore, 1989).